

## Density and Mechanical Properties of Sodium Borotellurite Glasses

Boya Nagendra<sup>1\*</sup>, Dr. K Narsimhulu<sup>2</sup>

### Author's Affiliations:

<sup>1</sup>Research Scholar,  
Rayalaseema University,  
Kurnool, Andhra Pradesh  
518002, India.

<sup>2</sup>Assistant Professor,  
Department of physics, SSA  
Govt First Grade College,  
Ballari, Andhra Pradesh  
515812, India.

### Corresponding author:

**Boya Nagendra,**  
Research Scholar,  
Rayalaseema University,  
Kurnool, Andhra Pradesh  
518002, India.

### E-mail:

nagendraboya@gmail.com

Received on 22.05.2018,

Accepted on 12.11.2018

### Abstract

Sodium borotellurite glasses in the system  $x\text{NaF}_2-(20-x) \text{Na}_2\text{O}-40\text{B}_2\text{O}_3-40\text{TeO}_2$  ( $0 < x < 20$  mol%) were prepared by melt quenching method. The density related parameters such as molar volume elastic constants and thermal properties were studied for present glasses with increasing  $\text{NaF}_2$  concentration. The results show that the calculated parameters strongly depend on increasing  $\text{NaF}_2$  concentration. The density reduction is due to fluorine ions entering interstitial spaces of the network and breaking B-O-Te bonds which results in decreasing density of the present glasses. The elastic constants of the present glasses were found to decrease with  $\text{NaF}_2$  content. This results in an increase of the discontinuity of the glass network. The thermodynamical parameters such as glass transition temperature and onset of crystallization temperature of the present glasses were found to decrease as a function of  $\text{NaF}_2$  concentration.

**Keywords:** Borotellurite Glasses, crystallization

### 1. Introduction

The study of tellurite glasses has been increased due to variety of applications in the field of optical communication due to their remarkable properties like high refractive index, high optical non-linearity and excellent infrared transmittance [1-3]. Compared to silica glasses tellurite glasses having higher Raman gain coefficients and also find application in Raman amplifiers and waveguides [4]. It has been reported that tellurite glasses are suitable to make photonic devices due to low melting temperature, thermal stability, low phonon energy and nonlinear refractive index, [5,6].

In the current world of technology glass material performance plays an important role. Among oxide glasses, borate glass is exclusive and can be used as thermal insulators and textile fiber glass.  $\text{B}_2\text{O}_3$  is the best glass former and borate glasses have good nonlinear optical properties [7]. Its existence in tellurite glasses results in a complex glass network consisting of  $\text{TeO}_4$ ,  $\text{TeO}_{3+1}$ ,  $\text{TeO}_3$ ,  $\text{BO}_4$  and  $\text{BO}_3$  structural units. The addition of  $\text{B}_2\text{O}_3$  into  $\text{TeO}_2$  glass, tellurite transforms  $\text{TeO}_4$  into  $\text{TeO}_{3+1}$  and  $\text{TeO}_3$  units and enhances the glass forming ability of  $\text{TeO}_2$ . The addition of  $\text{B}_2\text{O}_3$  also effects in decreasing B-O co-ordination with increase in  $\text{B}_2\text{O}_3$  concentration in borotellurite glasses [8]. Whereas, boron oxide ( $\text{B}_2\text{O}_3$ ) is an excellent material for combination with  $\text{TeO}_2$  as it improves the glass quality in terms of transparency, RE ions solubility, hardness and glass stability [9,10].

Presently Sodium based glasses are very attractive many scientists because of low melting and easy fabrication. The glasses have also extensive applications in the field of glass ceramics, layers for optical and electronic devices, thermal and mechanical sensors, reflecting windows, IR domes, and laser windows [11-14]. Sodium borosilicate glasses have a widespread interest in a number of fields such as bioactive glasses or the storage of nuclear waste [15]. They are chemically inert, mechanically strong, and resistant to thermal shocks; these properties explain their widespread usage in the glass industry.

The introduction of sodium with different glass former haven been reported in literature. The glassy system  $\text{Na}_2\text{O}-\text{B}_2\text{O}_3-\text{SiO}_2$  found wide application in various composite materials used in laser engineering and optoelectronics [16]. Antropova et al. studied thermophysical characteristics of glasses based on the  $\text{Na}_2\text{O}-\text{B}_2\text{O}_3-\text{SiO}_2$  system [17]. Pacaud et al. [18] also studied  $\text{Na}_2\text{O}-\text{B}_2\text{O}_3-\text{SiO}_2$  glasses from molecular simulation and conclude that the impact of sodium ions on the boron coordination at room temperature is in good agreement with experimental observations. Wakasugi et al. [19] studied Crystallization Tendency of  $\text{Na}_2\text{O}-\text{B}_2\text{O}_3-\text{Al}_2\text{O}_3$  glassy system. They have found that the glass stability increasing with increasing  $\text{Al}_2\text{O}_3$  concentration. Mansour [20] studied FTIR spectra binary sodium borate glasses containing  $\text{TeO}_2$ . It has been observed that introducing  $\text{TeO}_2$  into  $\text{Na}_2\text{O}-\text{B}_2\text{O}_3$  glasses may delay the expected loss of non-bridging oxygens (NBOs) in the complete glass network with the decreasing sodium oxide content.

Fluoride glasses are the most important materials for the optical fiber technology [24, 25] due to their improved infrared transmission characteristics. Fluoroborate glasses composition a vital role in the development of new optoelectronic devices due to their high ionic conductivity. Kamitsos and Karakassids [24] reported spectroscopic properties of fluoride containing sodium borate glasses and discussed the role of fluorine ions in the conducting properties. Shelby and Ortolano [26] prepared of  $\text{NaF}-\text{Na}_2\text{O}-\text{B}_2\text{O}_3$  glasses and studied the refractive index, density and glass transition temperatures of all glasses. Karunakaran et al. [27, 28] studied Structural, optical and thermal investigations of fluoroborate glasses doped with  $\text{Dy}^{3+}$  ions. The variation of optical properties discussed with  $\text{Dy}^{3+}$  ions. Karthikeyan et al. [29] also investigated Spectroscopic and glass transition of  $\text{Nd}^{3+}$  doped fluoroborate glasses.

Fluorine ion has almost the same radius as an oxygen ion, the possibility of substitution of the oxygen ions with fluorine ions is high, but the fluorine ions could also occupy interstitial positions. Moreover, fluorine has a greater electronegativity than oxygen which would reason the breakdown of the glass network structure, the glass transition and deformation temperatures would be likely to decrease with the substitution of fluoride ions in place of oxide ions. Several studies on the introduction of fluorine ions into oxide ions were reported for ternary sodium borate glasses [24,25,28]. Nearly all the studies are focused on the ternary borate system. There are no reports on introduction of fluorine ions into oxide ions in quaternary sodium borotellurite glasses. In the present work, an effort has been made for the preparation, physical and mechanical properties of  $x\text{NaF}_2 - (20-x) \text{Na}_2\text{O}-40\text{B}_2\text{O}_3-40\text{TeO}_2$  glasses.

## 2. Experimental

In the current study, the glass samples of composition  $x\text{NaF}_2 - (20-x)\text{Na}_2\text{O}-40\text{B}_2\text{O}_3-40\text{TeO}_2$  ( $0 < x < 20$  mol%) were ready by melt quench technique. High purity (99.99%) sodium fluoride ( $\text{NaF}_2$ ), sodium oxide ( $\text{Na}_2\text{O}$ ), tellurium oxide ( $\text{TeO}_2$ ) and Boron trioxide ( $\text{B}_2\text{O}_3$ ) (all Sigma Aldrich) were used as initial materials. A batch of 15 g of the above high purity chemicals in powder form was considered, well mixed and melted in a silica crucible in the temperature range  $1200-1250^\circ\text{C}$  subject on the glass composition in an electrical furnace for about 30 min. The melt was swirled frequently until a bubble free clear liquid was formed. The resulting melt was then transferred into a stainless steel mould warmed to  $200^\circ\text{C}$  and pressed with another steel disc conserved at the same temperature. All the glass samples were annealed at  $200^\circ\text{C}$  for a duration of about 12h. For samples taken from different regions of the bulk specimen, the absence of any Bragg peaks in the X-ray diffraction pattern complete that the ready glasses are amorphous.

The room temperature density ( $\rho$ ) of the glass was determined by the standard principle of Archimedes by means of xylene as the buoyant liquid. The density was calculated by the formula. The thermal performance of the glass samples was examined using a differential scanning calorimeter (Mettler-Toledo: TGA/DSC1/1600HT). Samples in the form of powder balancing about 15 mg were sealed in aluminum pans and scanned with a heating rate of 10°C/min from 30 to 600°C in dry nitrogen atmosphere. The glass transition temperature ( $T_g$ ) and the crystallization beginning temperature ( $T_x$ ) were determined based on the DSC curves using the onset method. The uncertainty in  $T_g$  and  $T_x$  are  $\pm 0.1^\circ\text{C}$ .

### 3. Results and discussion

#### 3.1 XRD

X-ray diffraction picture of the current glass samples are shown in Fig. 1. The Figure 1 shows no continuous or discrete sharp peaks but show wide halo, which reveals the features of amorphous glass structure.

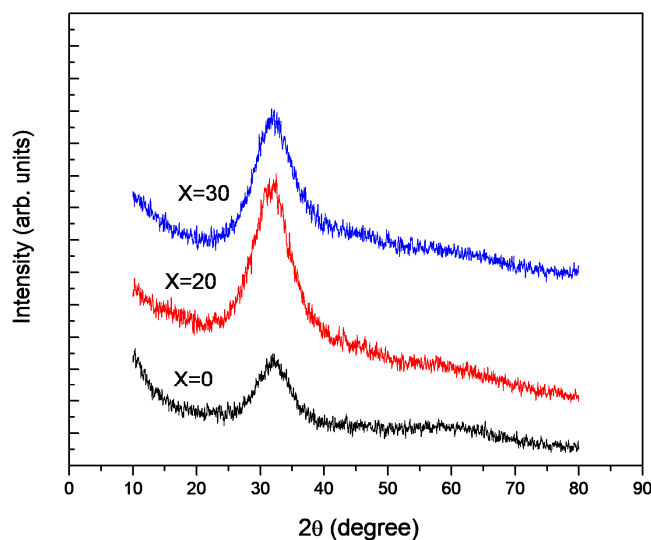


Figure 1: XRD spectra of present glasses

#### 3.2 Density

The density and molar volume was calculated by the formula

$$\rho = a * 0.86 / (a-b) \quad (1)$$

where a and b are the weights of the glass sample measured in air and xylene, respectively. The density of xylene at room temperature is 0.865 g/cc.

$$V_m = M / \rho \quad (2)$$

Where M is the average molecular weight of the glass and  $\rho$  is its density.

The density of the existing glass system varies from 3.944 to 3.824 g/cc and shown in table 1. Figure 2 shows the variation of density with NaF<sub>2</sub> concentration. The density reduction of the present glasses with NaF<sub>2</sub> concentration may be due to the low density of NaF<sub>2</sub> compared with that of NaO. The density decrease in the contemporary glasses can be described through the bond formation in present glasses. An significant chemical feature of Te atoms is their increasing valence from 3 to 4. But Boron has poor electron valence, when B<sub>2</sub>O<sub>3</sub> joint with TeO<sub>2</sub> when a modifier Na<sub>2</sub>O is added, the modifier ion may also be attracted towards BO<sub>3</sub> units leading to the construction of tetrahedral borate units or

it may be taken up by the  $\text{TeO}_2$  for construction to network structure [30]. Monsour [20] studied  $\text{Na}_2\text{O-B}_2\text{O}_3\text{-TeO}_2$  glass system through FTIR spectroscopy and confirm that that these glasses has high rich of B-O-Te bonds. In the present glasses when  $\text{NaF}_2$  replaced with  $\text{NaO}$ , fluorine ions will enters interstitial spaces of the network and breaking B-O-Te bonds which results decreasing density of the present glasses. In the present glass system, the variation of molar volume as a function of  $\text{NaF}_2$  content is also illustrated in figure 1. Since the behavior of molar volume mainly depends on the density of the glass and hence the variation of molar volume in these glasses is as expected.

**Table 1:**

Parameters	X=0	X=4	X=8	X=12	X=16	X=20
Density	3.944	3.914	3.886	3.859	3.835	3.824
Molar Volume	26.393	26.582	26.762	26.938	27.097	27.168
Ionic pacing density	0.546	0.539	0.533	0.525	0.518	0.514
Dissociation energy (K cal/cc)	14.380	14.234	14.088	13.942	13.796	13.650
Young's modulus (GPa)	157.115	153.399	149.868	146.391	143.064	140.267
Bulk modulus (GPa)	101.618	99.212	95.652	92.225	89.014	86.478
Shear modulus (GPa)	63.233	61.735	60.482	59.246	58.056	57.032
Poisson's ratio	0.245	0.242	0.238	0.235	0.232	0.229
<b>Thermal Properties</b>						
$T_g$	426.2	412.6	376.9	373.9	362.2	344.3
$T_x$	496.3	502.1	491.7	487.8	469.3	459.7
S	70.06	89.48	114.77	113.86	107.02	115.39

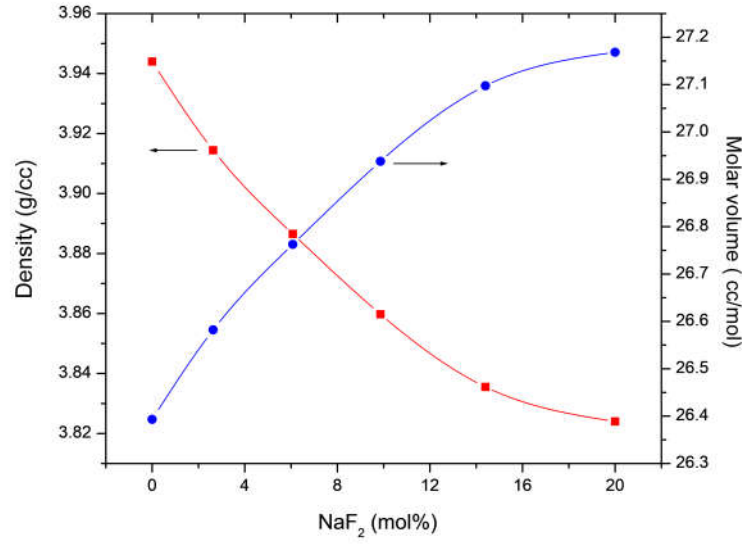


**Figure 2:** Density and Molar volume of  $x\text{NaF}_2 - (20-x)\text{Na}_2\text{O} - 40\text{B}_2\text{O}_3 - 40\text{TeO}_2$  glasses.

### 3.3 Elastic constants

Recently, Inaba and Fujino [31] described an experimental equation for ionic packing ratio, which is used to develop the density model. The ionic packing density  $V_t$  is expressed by

$$V_t = (\rho / M) \times \sum (V_i \times x_i) \quad (3)$$

Where  $M$  is molar weight (kg/mol),  $x_i$  is molar fraction (mol%),  $\rho$  is density (kg/m<sup>3</sup>) and  $V_i$  is packing density parameter (m<sup>3</sup>/mol).

For a typical glass composition  $4\text{NaF}_2 - 16\text{NaO} - 40\text{B}_2\text{O}_3 - 40\text{TeO}_2$ , the value of  $V_t$  is given by  $(1/26.8522) [(0.04)V_i(\text{NaF}_2) + (0.16)V_i(\text{NaO}) + (0.40)V_i(\text{B}_2\text{O}_3) + (0.40)V_i(\text{TeO}_2)]$ . The values of  $V_i(\text{NaF}_2) = 10 \times 10^{-6} \text{ m}^3/\text{mol}$ ,  $V_i(\text{Na}_2\text{O}) = 12.3 \times 10^{-6} \text{ m}^3/\text{mol}$ ,  $V_i(\text{TeO}_2) = 14.7 \times 10^{-6} \text{ m}^3/\text{mol}$  and  $V_i(\text{B}_2\text{O}_3) = 15.2 \times 10^{-6} \text{ m}^3/\text{mol}$  are used [31-33]. The calculated ionic packing density  $V_t$  of all the present glasses are summarized in table 1.

The elastic moduli of glasses may be calculated according to a model built upon the dissociation energy of the bonds and ionic radii of elements. This model was adopted by Makishima-Mackenzie [34, 35]. According to this model elastic constants is given by

$$G_t = \sum (x_i \times G_i) \quad (4)$$

$$E = 2 V_t G_t \quad (5)$$

$$K = 1.2 V_t E \quad (6)$$

$$S = 3 E K / (9 K - E) \quad (7)$$

$$\mu_{\text{cal}} = 0.5 - 1 / (7.2 V_t) \quad (8)$$

where  $G_i$  is the dissociation energy per unit volume of  $i^{\text{th}}$  oxide and  $x_i$  is the mol % of the  $i^{\text{th}}$  oxide.

The values of dissociation energy per unit volume  $G_i$  of various oxides used in the present study are  $G(\text{Na}_2\text{O})=8.90$  kcal/cc,  $G(\text{NaF}_2)=5.25$  kcal/cc,  $G(\text{TeO}_2)=12.85$  kcal/cc and  $G(\text{B}_2\text{O}_3) =18.6$  kcal/cc [36]. Using the above values, the dissociation energy  $G_i$ , the Young's modulus  $E$ , bulk modulus  $K$ , shear modulus  $S$  and Poisson's ratio  $\mu_{\text{cal}}$  of the present glass system were calculated and are presented in table 1.

Figure 3 explains the variation of Young's modulus and Figure 4 explains the variation of shear modulus and bulk modulus and as a function of  $\text{NaF}_2$  content in current glass system. From the Figures 3,4 it is clear that the elastic constants decreases with compositional parameter  $\text{NaF}_2$ .

In the existing study, the elastic moduli decrease with the increase in  $\text{NaF}_2$  content can be interpreted through the decrease in the dissociation energy per unit volume ( $G_i$ ) calculated according to Makishim-Mackenzie model [34, 35], indicating the decrease in bond strength and the rigidity.

Decreasing in elastic constants can also be explained by taking into account the relationship between the bulk and Young's moduli and the molar volume. The bulk modulus ( $K$ ) and the molar volume ( $V_m$ ) are related by the relation;  $KV_m^n = C$  [37] (where  $C$  is a constant). As stated earlier, the value of  $n$  for oxide glasses is 4 [38], and the variation of  $n$  in the bulk modulus-volume relationship is determined by the nature of the bonding, and the coordination polyhedra. When the volume change occurs without change in the nature of the bonding or change in the coordination polyhedra,  $\log(K)$  versus  $\log(V_m)$  plot in generally is linear. Thus the  $\log(K)$  versus  $\log(V_m)$  plot for the present glass system as shown in Figure 5, shows an increase in the molar volume associated with an expected decrease in bulk moduli. Thus the continuous substitution of  $\text{NaF}_2$  for  $\text{NaO}$  in the present glasses results in an increase of the discontinuity of the glass network. Such a decrease in both bulk and Young's moduli- volume relationship was observed in some other types of glasses [39,40].

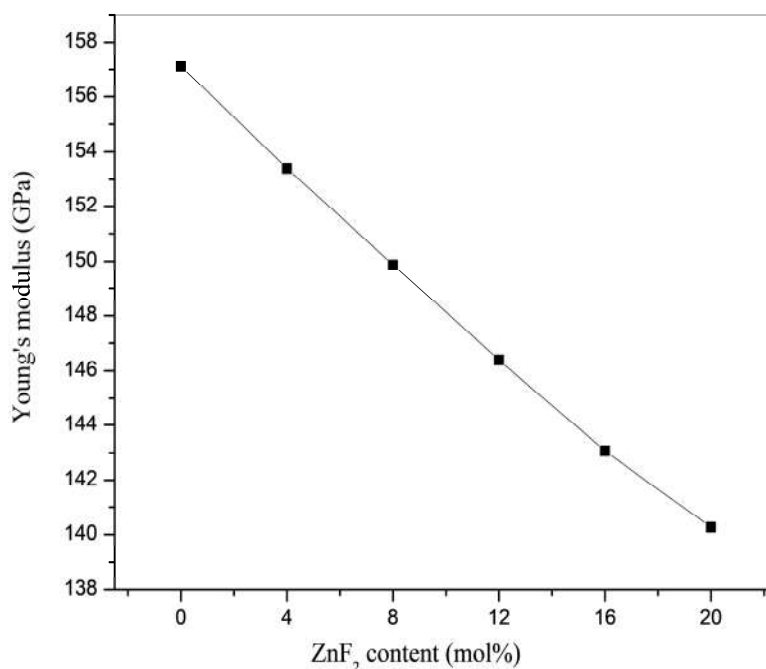
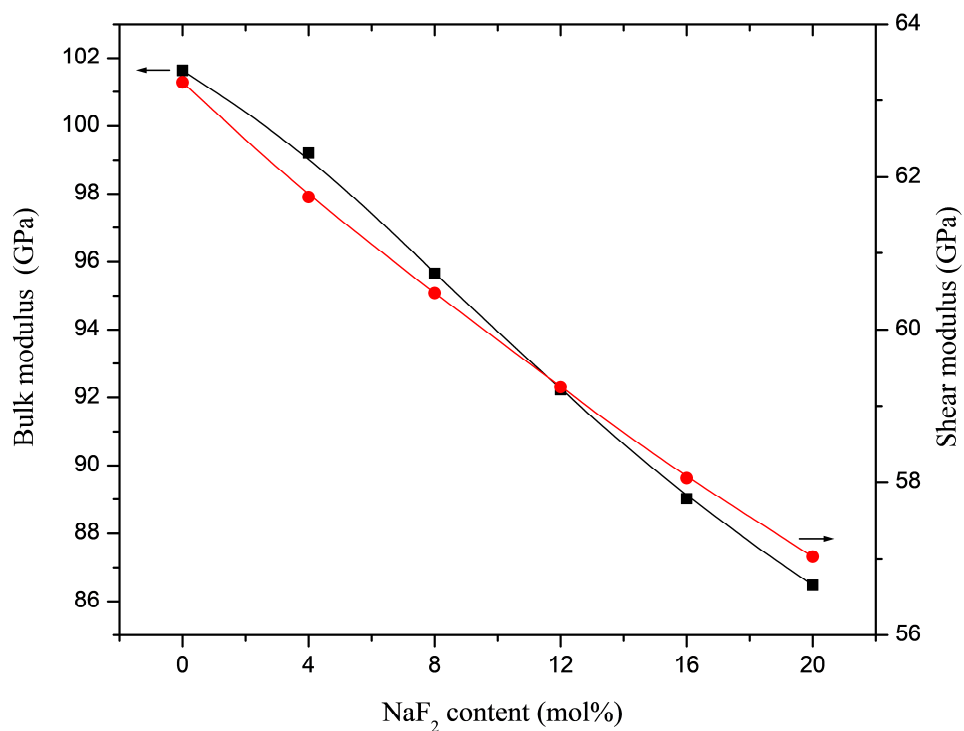
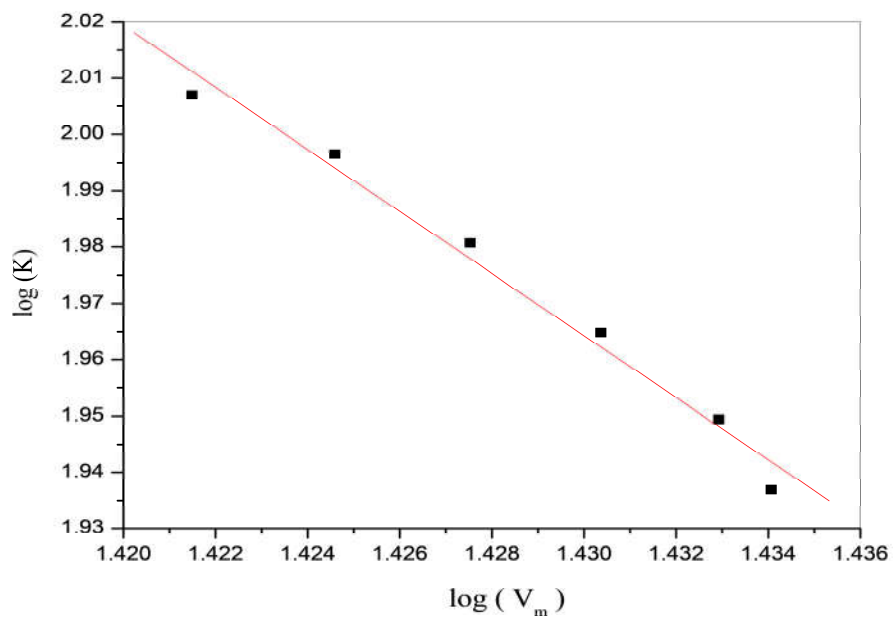


Figure 3: Young's modulus of the current glasses



**Figure 4:** Bulk and Shear modulus of the present glasses.



**Figure 5:**  $\log(K)$  versus  $\log(V_m)$  plot for the present glass system.

Figure 6 illustrates the variation of Poisson's ratio with  $\text{NaF}_2$  content in the present glass system. From the above figure it is observed that the Poisson's ratio  $\mu_{\text{cal}}$  decreases with glass composition. In present glass system the Poisson's ratio varies between 0.245 to 0.229.

It is known that Poisson's ratio is small if atoms are loosely packed in the oxide glass whereas tightly packed glass has a higher Poisson's ratio. In solid materials, the axial strain produced in the network is unaffected by the cross-links while the lateral strain is greatly decreased with increasing covalence of bonds [41]. Bridge and Higazy [42] have suggested a close correlation between Poisson's ratio and cross-link density which is defined as the number of bridging bonds per cation. According to Rao [43] Poisson's ratio depends on the dimensionality of the structure and cross-link density. A three dimensional network structure has lower Poisson's ratio than that of a two dimensional structure, since the number of bonds resisting a transverse deformation decreases in that order.

It is known that Poisson's ratio is affected by the changes in the cross-link density of the glass network. This means that as reported by Rajendran *et al* [38, 44], a high cross-link density has Poisson's ratio in the order of 0.1-0.2, while a low cross-link density has Poisson's ratio between 0.3 and 0.5. In the present glass systems, Poisson's ratio as shown in table 3.3 decreases and varies between 0.245 to 0.229. The values of the Poisson's ratio suggests that the present glasses have a low cross-link density. Some structural readjustments are presumed to take place when  $\text{NaO}$  is substituted by  $\text{NaF}_2$

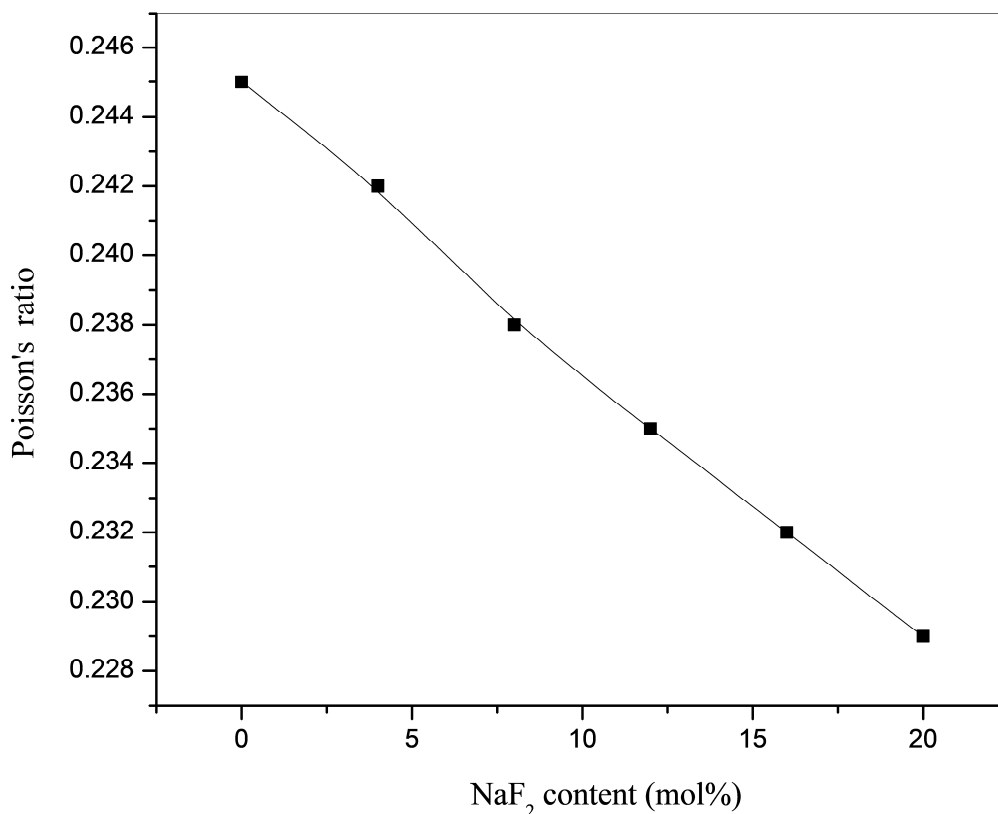


**Figure 6:** Variation of Poisson's ratio with  $\text{NaF}_2$  content in the present glass



### 3.4. Differential scanning calorimetry

The differential scanning calorimetry (DSC) is used to characterize the glass and to determine the thermodynamical parameters. The DSC thermograms of all the glass samples are shown in Figure 7. The glass transition temperatures ( $T_g$ ) and onset of crystallization temperature ( $T_c$ ) were determined based on the DSC curves using the onset method. The glass transition temperature  $T_g$  was taken as the temperature corresponding to the intersection of the two linear portions adjoining the transition elbow in the DSC traces. The uncertainty in  $T_g$  and  $T_c$  is  $\pm 0.1^\circ\text{C}$ . The glass stability  $S$  was determined by using the formula  $S = T_c - T_g$ . The determined values of  $T_g$ ,  $T_c$  and  $S$  were presented table 2. The glass transition temperature decreases from 426.2 to  $344.3^\circ\text{C}$ . The crystallization onset temperature is also shifted to lower temperature range from 496.3 to  $459.7^\circ\text{C}$ . The glass stability ( $S$ ) varies in the range 70 to  $115^\circ\text{C}$  and is large enough to obtain stable glass. Figure 8 plots the variation of  $T_g$ ,  $T_c$  and  $S$  as a function of  $\text{NaF}_2$  content. The reduction in glass transition temperature and onset of crystallization can be summarized as follows:

The reduction in glass transition temperature in present glass may be due to the fact that the fluorine has a higher electronegative than oxygen, it would be expected that the substitution of fluoride ions for oxide ions decrease glass transition temperature and deformation temperature. Since two fluoride ions are substituted for an oxide ion, which causes the breakdown of the glass network structure and the fluorine atoms are introduced in oxide network can be considered not to act as bridge between two tellurium atoms because of single valence of fluorine. Breaking the oxide network, the cross linking degree of the glass former could be reduced which results in decrease of both  $T_g$  and  $T_c$ .

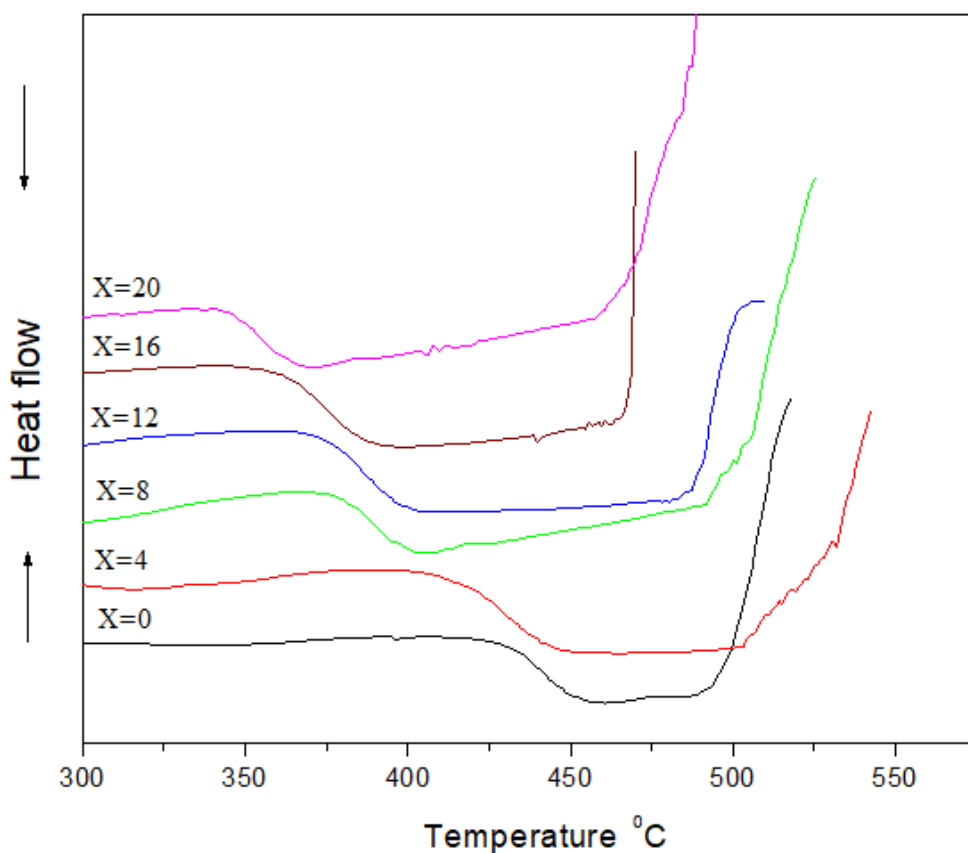
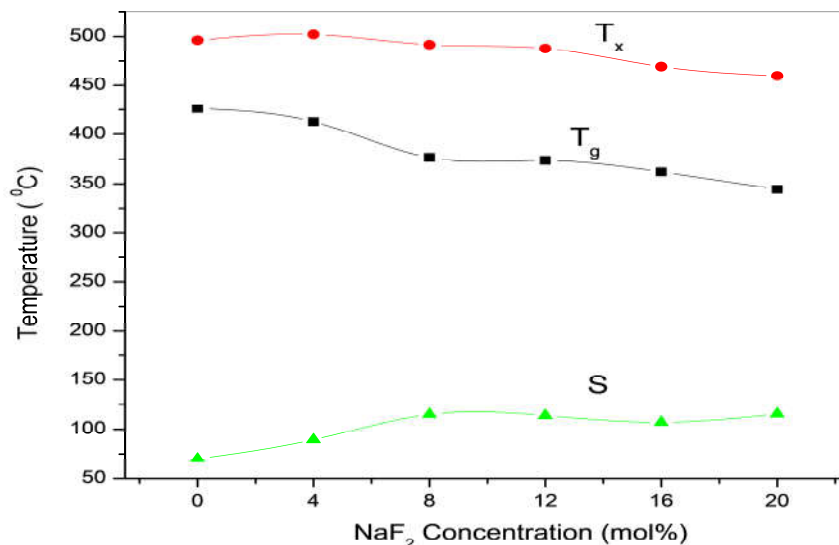


Figure 7: DSC thermograms of  $x\text{NaF}_2-(20-x)\text{Na}_2\text{O}-40\text{B}_2\text{O}_3-40\text{TeO}_2$  glasses.



**Figure 8:** Variation of  $T_g$ ,  $T_c$  and  $S$  as a function of  $\text{NaF}_2$  content

#### 4. Conclusions

The following conclusions are drawn from the study of various physical properties on  $x\text{NaF}_2$ -(20-x)  $\text{Na}_2\text{O}$ -40 $\text{B}_2\text{O}_3$ -40 $\text{TeO}_2$  glasses.

- The room temperature density of  $x\text{NaF}_2$  -(20-x) $\text{Na}_2\text{O}$ -40 $\text{B}_2\text{O}_3$ -40 $\text{TeO}_2$  glasses decreased non linearly as a function of  $\text{NaF}_2$  content and the density reduction is due fluorine ions will enters interstitial spaces of the network and breaking B-O-Te bonds which results decreasing density of the present glasses
- Young's modulus, bulk modulus, shear modulus and Poisson's ratio of the present glasses were determined using the density data and the dissociation energy per unit volume. The elastic constants of the present glasses were found to decrease with  $\text{NaF}_2$  content. This results in an increase of the discontinuity of the glass network.
- The Poisson's ratio of the present glass system decreases from 0.245 to 0.229 proposing that the current glasses have a low cross link density.
- The thermodynamically parameters such as glass transition temperature and onset of crystallization temperature of the present glasses and were found to decrease as a function of  $\text{NaF}_2$  concentration.

#### References

1. H. Nasu, O. Matsushita, K. Kamiya, H. Kobayashi and K.i. Kubodera, Journal of Non-Crystalline Solids 124, 275-277 (1990).
2. M.H. Bhat, M. Kandavel, M. Ganguli and K.J. Rao, Bulletin of Materials Science 27, 189-198 (2004).
3. Shaik kareem Ahmmad, M.A. Samee, A. Edukondalu, Syed Rahman, Results in physics 2 (2012) 175-181
4. P. Gayathri Pavani, K. Sadhana and V. Chandra Mouli, Physica B: Condensed Matter 406, 1242-1247 (2011).
5. M. N. Azlan, M. K. Halimah, S. Z. Shafinas, and W. M. Daud, Materials Express, 5 (2015) 211-218.
6. I. Jlassi, H. Elhouichet, and M. Ferid, 46 2011 (3) 806-812.
7. P. Becker, Adv. Mater. 10 (1999) 979-992.
8. N. Kaur, A. Khanna, J. Non-Cryst. Solids 404 (2014) 116-123.

9. A.V. Deepa, M. Priya, S. Suresh, 11 (5) (2016) 57–63.
10. YANG Yanmin, LIU Yanzhou, CAI Peiqing, Ramzi , Hyo Jin Seo, 33 (2015) 939.
11. K. Gerth, C. Russesl, J. Non-Cryst. Solids 221 (1997) 10.
12. R.A.F. El-Mallaway, Tellurite Glasses Handbook: Properties and Data, CRC, BocaRaton, FL, 2002.
13. J.S. Wang, E.M. Vogel, E. Snitzer, Opt. Mater. 3 (1994) 187.
14. S.H. Kim, T. Yoko, S. Sakka, J. Am. Ceram. Soc. 76 (1993) 865.
15. M. J. Plodinec, Glass Technol. 41, 186–192 (2000).
16. K. Meshkovski., *Composite Optical Materials Based on Porous Matrices* St. Petersburg, 1998.
17. T. V. Antropova, S. V. Stolyar, and V. L. Stolyarova
18. Fabien Pacaud, Jean-Marc Delaye, , Thibault Charpentier, Laurent Cormier, Mathieu Salanne The Journal of Chemical Physics 147, (2017) 161711.
19. Takashi Wakasugi, Rikuo Om, and Jiro Fukunaga, J. American ceramic society 75[11]3129
20. E. Mansour, Journal of Molecular Structure 1014 (2012) 1–6
21. A. Lecoq, M. Poulain, J. Non-Cryst. Solids 41 (1980) 209.
22. M.C. Briereley, C.A. Millar, Electron. Lett. 24 (1988) 438.
23. Y. Ohishi, M. Yamada, T. Kanamori, S. Suda, Opt. Lett. 22 (1997) 1235.
24. Kamitsos and Karakassids, solid state ionics, 28-30 (1988) 783-787.
25. Shantala D patil, V. M jail, R.V Anavekar, Bull. Mater. Sci, 31 (2008) 631–634.
26. J.E. Shelby, R.L. Ortolano, Phys. Chem. Glasses 31 (1990) 25.
27. R.T.Karunakaran, K.Marimuthu, S.Surendra Babu, S. Arumugam, Physica B 404 (2009) 3995–4000.
28. R.T.Karunakaran, K.Marimuthu, S.Surendra Babu, S.Arumugam, Journal of Luminescence 130 (2010) 1067-1072
29. B. Karthikeyana, S. Mohan, Materials Research Bulletin 39 (2004) 1507–1515.
30. V.C. Veeranna Gowda, C. Narayana Reddy, K.C. Radha, R.V. Anavekar, J Etourneau, K.J. Rao, J. Non-Cryst. Solids 353 (2007) 1150–1163.
31. S. Inaba, S. Fujino, J. Am. Ceram. Soc. 93 (2010) 217.
32. R.D. Shannon, C.T. Prewitt, Acta Crystallogr B 25 (1969) 925
33. R.D. Shannon, C.T. Prewitt, Acta Crystallogr B 26 (1970) 1046
34. A. Makishima, J.D. Mackenzie, J. Non-Cryst. Solids 12 (1973) 35
35. A. Makishima, J.D. Mackenzie, J. Non-Cryst. Solids 17 (1975) 147
36. S. Inaba, S. Oda, K. Morinaga, J. Non-Cryst. Solids 325 (2003) 258
37. E. Gopal, T. Mukuntan, J. Philip, S. Sathish, Pramana, J. Phys. 28 (5) (1987) 471
38. V. Rajendran, N. Palanivelu, B.K. Chaudhuri, K. Goswami, J. Non-Cryst. Solids 320 (2003) 195
39. Y.B. Saddeek, J. Alloys and Compounds 467 (2009) 14.
40. M.S. Gaafar, H.A. Afifi, M.M. Mekawy, Physica B 404 (2009) 1668.
41. N. D. Patel, D. N. Waters, Phys. Stat. Sol. (a) 77 (1983) 655
42. B. Bridge, A. A. Higazy, Phys. Chem. Glasses 27 (1986) 1
43. K. Rao, Structural Chemistry of Glasses, Elsevier, North Holland, 2002.
44. V. Rajendran, N. Palanivelu, D.K.Modak, B.K. Chaudhuri, Phys. Stat. Sol. A 180 (2000) 467
45. Shaik Kareem Ahmmad, M. A. Samee, S. M. Taqiullah, and Syed Rahman, AIP Conference Proceedings 1591, 730 (2014);